



Calhoun: The NPS Institutional Archive DSpace Repository

Theses and Dissertations

1. Thesis and Dissertation Collection, all items

1975

A comparison of optimal control theory predictions with actual pilot performance in a helicopter longitudinal tracking task.

Wheat, Luther William

Monterey, California. Naval Postgraduate School

<http://hdl.handle.net/10945/20781>

Downloaded from NPS Archive: Calhoun



<http://www.nps.edu/library>

Calhoun is the Naval Postgraduate School's public access digital repository for research materials and institutional publications created by the NPS community.

Calhoun is named for Professor of Mathematics Guy K. Calhoun, NPS's first appointed -- and published -- scholarly author.

Dudley Knox Library / Naval Postgraduate School
411 Dyer Road / 1 University Circle
Monterey, California USA 93943

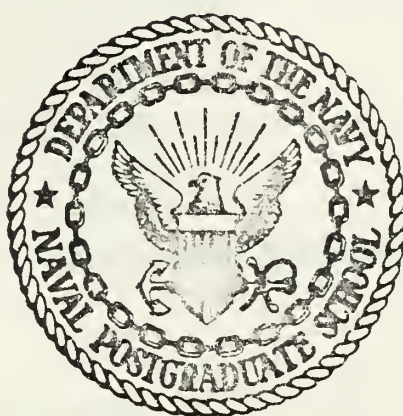
A COMPARISON OF OPTIMAL CONTROL THEORY
PREDICTIONS WITH ACTUAL PILOT PERFORMANCE
IN A HELICOPTER LONGITUDINAL TRACKING TASK

Luther William Wheat

DUDLEY KNOX LIBRARY
NAVAL POSTGRADUATE SCHOOL
MONTEREY, CALIFORNIA 93940

NAVAL POSTGRADUATE SCHOOL

Monterey, California



THESIS

A COMPARISON OF OPTIMAL CONTROL THEORY
PREDICTIONS WITH ACTUAL PILOT PERFORMANCE
IN A HELICOPTER LONGITUDINAL TRACKING TASK

by

Luther William Wheat

Thesis Advisor:

R. A. Hess

Approved for public release; distribution unlimited.

T169612

effectiveness of each display as well as the predictive power of the pilot model.

A Comparison of Optimal Control Theory
Predictions With Actual Pilot Performance
In A Helicopter Longitudinal Tracking Task

by

Luther William Wheat
Lieutenant, United States Navy
A.B., Georgia State College, 1968

Submitted in partial fulfillment of the
requirements for the degree of

MASTER OF SCIENCE IN AERONAUTICAL ENGINEERING

from the

NAVAL POSTGRADUATE SCHOOL
June 1975

ABSTRACT

A fixed base helicopter simulation was implemented which may be easily altered to represent a variety of conventional single rotor aircraft. Test subjects performed 90-second tracking tasks utilizing two cockpit displays for longitudinal control during landing approach. The performance data generated were compared with predicted values from an optimal pilot modeling technique. Tentative conclusions were drawn as to the effectiveness of each display as well as the predictive power of the pilot model.

TABLE OF CONTENTS

I.	INTRODUCTION-----	10
II.	METHOD OF INVESTIGATION-----	11
III.	APPARATUS AND PROCEDURES-----	11
IV.	OPTIMAL PILOT MODEL AND PREDICTIONS-----	15
V.	RESULTS-----	17
VI.	CONCLUSIONS-----	18
	APPENDIX A - THE DIGITAL PROGRAM-----	32
	APPENDIX B - THE ANALOG PROGRAM-----	40
	LIST OF REFERENCES-----	42
	INITIAL DISTRIBUTION LIST-----	43

LIST OF TABLES

I.	UH-1H LONGITUDINAL DERIVATIVES AS USED IN SIMULATION-----	20
II.	TURBULENCE MODELS-----	21
III.	MODEL PERFORMANCE PREDICTIONS-----	22
IV.	SIMULATION PERFORMANCE DATA-----	23

LIST OF FIGURES

1. Lines of Communication-----	24
2. Apparatus-----	25
3. Cockpit Display-----	26
4. Optimal Pilot Model-----	27
5. Performance Values, Subject A-----	28
6. Performance Values, Subject B-----	29
7. Control Motion, Baseline Display-----	30
8. Control Motion, Quickened Display-----	31

LIST OF SYMBOLS

g	Acceleration of gravity, ft/sec ² .
I_y	Aircraft mass moment of inertia about y stability axis, slug-ft ² .
M	Moment about y stability axis, ft-lbs.
m	Aircraft mass, slugs.
q	Aircraft angular rate about y stability axis, radians/sec.
U_o	Aircraft reference flight velocity, ft/sec.
u	Perturbation flight velocity along x stability axis, ft/sec.
u_g	Horizontal wind gust velocity, ft/sec.
w	Perturbation flight velocity along z stability axis, ft/sec.
w_g	Vertical wind gust velocity, ft/sec.
X	Force component along x stability axis, lbs.
Z	Force component along z stability axis, lbs.
δ_b	Cyclic pitch control input, ft. displacement at the pilot's hand.
δ_c	Collective pitch control input, ft. displacement at the pilot's hand.
θ	Perturbation pitch angle about y axis, radians.

The following stability derivatives are defined for a reference flight condition in stability axes.

$$X_q = \frac{1}{m} \frac{\partial X}{\partial q}$$

$$X_u = \frac{1}{m} \frac{\partial X}{\partial u}$$

$$X_w = \frac{1}{m} \frac{\partial X}{\partial w}$$

$$X_{\delta_b} = \frac{1}{m} \frac{\partial X}{\partial \delta}_b$$

$$Z_q = \frac{1}{m} \frac{\partial Z}{\partial q}$$

$$Z_u = \frac{1}{m} \frac{\partial Z}{\partial u}$$

$$Z_w = \frac{1}{m} \frac{\partial Z}{\partial w}$$

$$Z_{\delta_b} = \frac{1}{m} \frac{\partial Z}{\partial \delta}_b$$

$$Z_{\delta_c} = \frac{1}{m} \frac{\partial Z}{\partial \delta}_c$$

$$M_q = \frac{1}{I_y} \frac{\partial M}{\partial q}$$

$$M_u = \frac{1}{I_y} \frac{\partial M}{\partial u}$$

$$M_w = \frac{1}{I_y} \frac{\partial M}{\partial w}$$

$$M_{\dot{w}} = \frac{1}{I_y} \frac{\partial M}{\partial \dot{w}}$$

$$M_{\delta_b} = \frac{1}{I_y} \frac{\partial M}{\partial \delta}_b$$

$$M_{\delta_c} = \frac{1}{I_y} \frac{\partial M}{\partial \delta}_c$$

I. INTRODUCTION

The use of vertical take-off and landing aircraft has increased significantly in both military and civil application. Helicopter flight under instrument flight rules has been accomplished on a routine basis for quite a while but low speed and terminal operations still require visual references outside the aircraft. The military services have had some success in low speed instrument flight but it is generally conceded that much work needs to be done in the area of cockpit information systems. One popular approach has been the use of electronic displays utilizing cathode-ray-tubes which have the advantage of almost unlimited flexibility in format and symbolism (References 1 and 2). Additionally, extensive work has been done in the field of pilot modeling and pilot-in-the-loop system performance (Ref.3); but in order to optimize pilot performance it is necessary to consider the nature and extent of information presented to the pilot. This project was aimed at the construction of a fixed base helicopter flight simulator and the comparison of real pilot performance with pilot model predictions under a limited range of conditions and using two visual displays.

II. METHOD OF INVESTIGATION

A helicopter simulation was constructed to represent the longitudinal flight dynamics of an unaugmented (i.e., without the usual mechanical stabilization bar) UH-1H helicopter. A fore and aft moving control stick provided cyclic pitch control inputs and a collective pitch lever produced power commands. A hybrid computer gave real time solutions to the helicopter equations of motion, generated each of two cockpit displays, and computed performance data. Performance values for each display mode were analytically predicted using optimal pilot modeling techniques and compared with simulation data for two test subjects.

III. APPARATUS AND PROCEDURES

The longitudinal motion of a helicopter can be described by the following equations of motion:

$$\dot{u} = X_u u + X_w w + X_q q - g\theta + X_{\delta_b} \delta_b + X_{\delta_c} \delta_c - X_u u_g - X_w w_g$$

$$\dot{w} = Z_u u + Z_w w + (U_o + Z_q)q + Z_{\delta_b} \delta_b + Z_{\delta_c} \delta_c - Z_u u_g - Z_w w_g$$

$$\dot{q} = (M_u + M_w Z_u)u + (M_w + M_w Z_w)w + (M_q + M_w (U_o + Z_q))q + (M_{\delta_b} + M_w Z_{\delta_b})\delta_b +$$

$$+ (M_{\delta_c} + M_w Z_{\delta_c})\delta_c - (M_u + M_w Z_u)u_g - (M_w + M_w Z_w)w_g$$

$$\dot{\theta} = q$$

$$\dot{h} = -w + U_o \theta$$

δ_b represents cyclic control input, δ_c collective input, and u_g and w_g horizontal and vertical wind gust velocities. Table I lists the stability derivative values used in this simulation. The equations above incorporate the following simplifying assumptions:

1. The vehicle has been idealized as a rigid airframe to which is attached a rotor.
2. The rotor is described by its tip path plane whose orientation determines propulsive and aerodynamic forces and moments.
3. No rotor degree of freedom is considered other than control inputs which serve to describe instantaneous tip path plane orientation.
4. Coupling between longitudinal and lateral motion has been ignored.
5. Motion has been linearized as small perturbations about a predetermined reference flight path.

The hybrid computer used consisted of a Scientific Data Systems SDS 9300 digital computer, A Comcor CI-5000 analog computer, and an Adage AGT-10 stroke written graphics processor, as illustrated in Figure 1. The digital computer was used to control the analog and graphics processor and to generate performance data. A program listing is found in Appendix A. In addition to the two display modes to be

described, provision has been made for the inclusion of flight director symbolism in a third display mode for future study. The analog computer gave solutions to the equations of motion in real time (Appendix B), and the graphics processor displayed textual and graphic information on a cathode ray tube in front of the test subject. Pilot control inputs were made directly to the analog using electrical voltage signals. The spring restrained cyclic stick operated a gear driven potentiometer and was linear in both force and displacement. The collective lever was unrestrained except for a friction brake and also used a gear driven potentiometer to generate a signal linear in displacement. The friction brake required a slight breakout force. Figure 2 shows the physical arrangement of the apparatus.

Atmospheric turbulence was modeled by a sum of sine waves:

$$u_g = \sum_{i=1}^5 A_i \sin \omega_i t, \text{ where } \begin{array}{lll} A_1 = 4.472 & \omega_1 = 0.070 \\ A_2 = 3.536 & \omega_2 = 0.210 \\ A_3 = 2.236 & \omega_3 = 0.350 \\ A_4 = 2.738 & \omega_4 = 0.768 \\ A_5 = 2.236 & \omega_5 = 1.765 \end{array}$$

and similarly,

$$w_g = \sum_{i=1}^5 A_i \sin \omega_i t, \text{ where } \begin{array}{lll} A_1 = 4.472 & \omega_1 = 0.420 \\ A_2 = 3.536 & \omega_2 = 1.260 \\ A_3 = 2.236 & \omega_3 = 2.100 \\ A_4 = 2.738 & \omega_4 = 4.608 \\ A_5 = 2.236 & \omega_5 = 10.050 \end{array}$$

The amplitudes and frequencies above were chosen so that the integration over ω of the power spectral densities closely approximated that for the turbulence spectra shown in Table II (Ref. 4). The advantage of this turbulence representation is that it is repeatable, has a mean value of zero, and appears completely random to the test subject.

Two different displays were presented to the test subjects for evaluation. The first was basically a real world display similar to current instrument installations and consisted of a horizon bar and aircraft reference for pitch control along with a glideslope deviation indicator. Airspeed deviation was provided by angular displacement of the aircraft reference "wings." The second display had symbolism identical to the baseline display but was quickened with rate information according to the equations:

$$\theta_{\text{quick}} = \theta + k_{\dot{\theta}} \dot{\theta}$$

$$h_{\text{quick}} = h + k_{\dot{h}} \dot{h} .$$

The quickening gains, $k_{\dot{\theta}}$ and $k_{\dot{h}}$, were simple pure gain approximations to the pilot transfer functions obtained in the modeling procedure. The display, shown in Figure 3, was 6 1/2 inches wide and 7 inches high. The nominal eye-to-display distance was 2 1/2 feet.

After considerable informal training, each subject received a formal training session in which he used the baseline and quickened display for 90 second runs each. In the

formal data sessions, each subject used each display for ten 90 second runs. The data sessions went as follows:

The baseline was flown for seven runs, followed by the quickened for seven. Then the quickened was flown for three runs followed by the baseline for three. Five of the "best" runs for each display were then selected. For ten data runs with each display, mean scores were computed for each of the root mean square performance measures (u , $\dot{\theta}$, θ , h , δ_b , δ_c). Then each RMS score for each display and run was normalized by dividing it with the respective mean RMS score. The normalized RMS scores were then summed to provide a single scalar index of performance for each display and run.

The data in Table IV represent the means and standard deviations of the RMS scores for the runs with the five lowest indices of performance for each display.

Figures 5 and 6 graphically portray the more pertinent performance data of Table IV for subject A (non-pilot) and subject B (pilot). Also indicated are the model predictions which best correlate with the data, i.e. $F = 0.25$.

IV. OPTIMAL PILOT MODEL AND PREDICTIONS

The analytic pilot model is shown schematically in Figure 4, and is basically the same as that offered by Kleinman and Baron (Ref. 5). This optimal pilot model includes the following assumptions:

1. Subject to inherent limitations, the well trained and motivated pilot behaves in an optimal manner.
2. With certain modifications, the solution to an optimal linear control and estimation problem will predict the pilot's control characteristics. These modifications are:
 - a. A pure time delay is included in each of the pilot's control outputs.
 - b. Each neuromuscular output system may be modeled as a first order lag.
 - c. Each variable that the pilot observes is assumed to contain pilot induced additive white noise which scales with the variance of the observed variable.
 - d. Each control output is assumed to contain pilot induced additive white noise which scales with the variance of the control.
 - e. The pilot is able to perceive the first derivative of a variable, also noise contaminated, but no higher derivative.

The index of performance for the optimization procedure was chosen subjectively by the analyst to represent the task objectives as perceived by the pilot. Model performance predictions are given in Table III for each of the displays. The parameter F represents the fraction of the pilot's attention devoted to the control task as a whole. For example, $F = 0.25$ suggests that 25% of the pilot's attention is devoted to control and 75% is dedicated to non-control activity such as communication, etc.

V. RESULTS

Table IV lists the root mean square performance data. Figures 5 and 6 give a graphical comparison of the most pertinent performance measures and the model predictions that best correlate with the data ($F = 0.25$). For each subject, the mean value is indicated, as well as plus and minus one standard deviation. In each case the pilot model predicted performance with a fair degree of accuracy. Additionally, the model predicted improvement for each performance measure using the quickened display, and the test subjects verified this prediction. However, the magnitude of performance improvement was greater in each case than was anticipated. It is possible that the task as perceived by the pilot may not be the same for each display mode. The task as understood may be to keep the deviation symbols within a finite distance, say $1/8"$, of their nominal position, and indeed there may exist a threshold of error below which the pilot makes no control input at all. Since the gains driving the deviation symbolism vary considerably between modes, each display then defines a new task. One possible arrangement would be to provide additional symbolism for the task variables, i.e. airspeed and glideslope deviations, which would be common between modes.

The dramatic reduction in cyclic motion, δ_b , was not predicted by the model. Typical time histories of cyclic

motion, Figures 7 and 8, show the nature of this improvement. Again the task defined by the display mode, in this case pitch attitude control, may be different. For both subjects, glideslope deviation control was poorest in comparison with model predictions, which suggests that more pilot attention was given to attitude/airspeed control than to the glideslope. Furthermore, collective motion was less for both subjects than was predicted. While the cyclic input was of a continuous nature, collective inputs were a series of steps (Figures 7 and 8) in each case. Such control action probably represents a wait and see technique used by pilots as a result of the lag in collective response. This phenomenon may in part explain the discrepancy between predicted and measured glideslope deviations since the optimal control model did not address this type of control motion.

Pilot comments indicated that the quickened display was more fatiguing than the baseline and represented an increase in pilot workload. Unfortunately, no measure of pilot workload, such as number of control inputs per minute, was recorded. Furthermore, no objective measure of the "well trained and motivated" assumption was available for each subject.

VI. CONCLUSIONS

The use of quickening in the cockpit display significantly reduced control motion and improved pilot performance. The predictive power of the optimal pilot model seemed adequate

even though this report represents only a first iteration. The quantitative quality of the model should improve as adjustments are made. The model index of performance can be adjusted to account for the pilot's apparent greater concern with pitch attitude/rate deviations as compared with altitude/rate deviations. In addition, the displays could be revised to eliminate any variation in the task presented to the pilot. As the control theoretic pilot model is refined and validated through testing it should become a valuable tool in the development of cockpit information systems and the expanded utility of the helicopter.

TABLE I

UH-1H LONGITUDINAL DERIVATIVES AS USED IN SIMULATION

X_u	= -0.11985	1/sec
X_w	= 0.35800	1/sec
X_q	= 1.9359	ft/sec
Z_u	= 0.28007	1/sec
Z_w	= -1.0775	1/sec
Z_q	= -1.4597	ft/sec
M_u	= 0.0058048	1/sec-ft
M_w	= -0.0030342	1/sec-ft
M_q	= -0.45465	1/sec
$M_{\dot{w}}$	= 0.0	1/ft
$X_{\delta b}$	= -3.4680	$1/\text{sec}^2$
$X_{\delta c}$	= 59.688	$1/\text{sec}^2$
$Z_{\delta b}$	= 48.486	$1/\text{sec}^2$
$Z_{\delta c}$	= -176.13	$1/\text{sec}^2$
$M_{\delta b}$	= -1.5757	$1/\text{ft}\cdot\text{sec}^2$
$M_{\delta c}$	= 0.0	$1/\text{ft}\cdot\text{sec}^2$

TABLE II
TURBULENCE MODELS

Vertical Turbulence

$$\Phi_{wgwg}(\omega) = \frac{2\sigma_w^2 L_w}{U_o} \frac{1}{1 + (\frac{L_w \omega}{U_o})^2} \text{ ft}^2 \text{ rad/sec}^2$$

$$\sigma_w = 5 \text{ ft/sec}$$

$$L_w = 100 \text{ ft}$$

$$U_o = 60 \text{ knots (101.3 ft/sec)}$$

Horizontal Turbulence

$$\Phi_{ugug}(\omega) = \frac{2\sigma_u^2 L_u}{U_o} \frac{1}{1 + (\frac{L_u \omega}{U_o})^2} \text{ ft}^2 \text{ rad/sec}^2$$

$$\sigma_u = 5 \text{ ft/sec}$$

$$L_u = 600 \text{ ft}$$

TABLE III
MODEL PERFORMANCE PREDICTIONS

F	Baseline Display			Quickened Display		
	1.0	0.5	0.25	1.0	0.5	0.25
σ_u (ft/sec)	.881	1.50	2.69	.666	1.23	2.45
σ_w (ft/sec)	2.94	3.75	5.11	2.24	3.02	4.39
$\sigma_{\dot{\theta}}$ (rad/sec)	.0109	.0147	.0204	.00829	.0118	.0178
σ_{θ} (rad)	.0104	.0158	.0259	.00795	.0128	.0231
σ_h (ft)	1.81	2.55	4.01	1.34	2.01	3.36
σ_{δ_B} (ft)	.0276	.0300	.0335	.0256	.0277	.0311
σ_{δ_C} (ft)	.0513	.0569	.0675	.0460	.0511	.0611

TABLE IV
SIMULATION PERFORMANCE DATA

Subject	<u>Baseline</u>		<u>Quickened</u>	
	1	2	1	2
σ_u (ft/sec)	5.58† 1.55††	2.60 .627	3.91 .653	1.86 .713
$\sigma_{\dot{\theta}}$ (rad/sec)	.0505 .00482	.0269 .00291	.0169 .00159	.0121 .00134
σ_{θ} (rad)	.0471 .00462	.0292 .00403	.0182 .00614	.0197 .00389
σ_h (ft)	9.31 1.04	5.51 .423	6.88 .949	4.79 .902
σ_{δ_b} (ft)	.0534 .00522	.0259 .00335	.0247 .00269	.0127 .00125
σ_{δ_c} (ft)	.0529 .00642	.0373 .00712	.0401 .00514	.0292 .00501

† mean

†† standard deviation

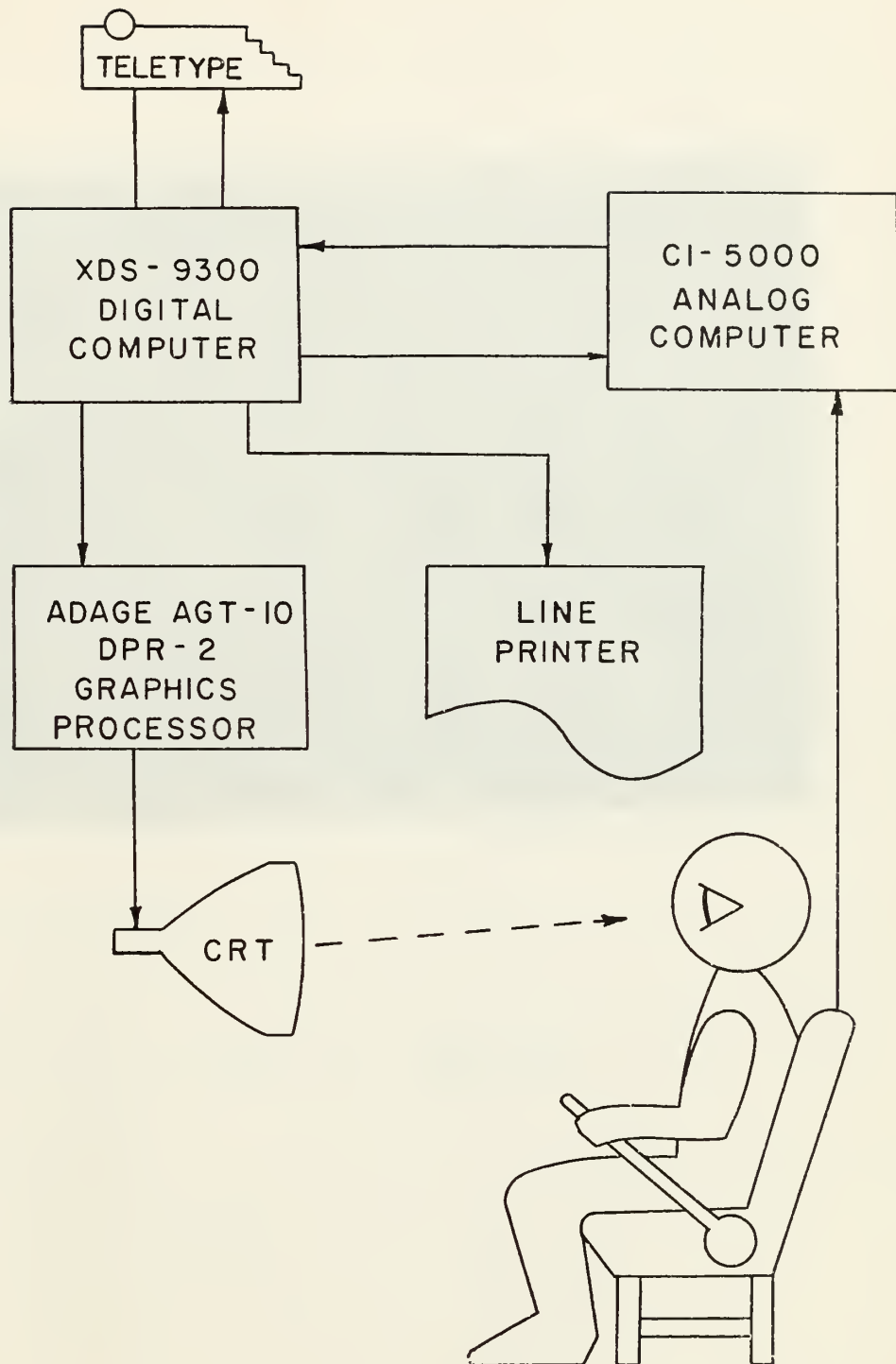


Figure 1. Lines of communication.

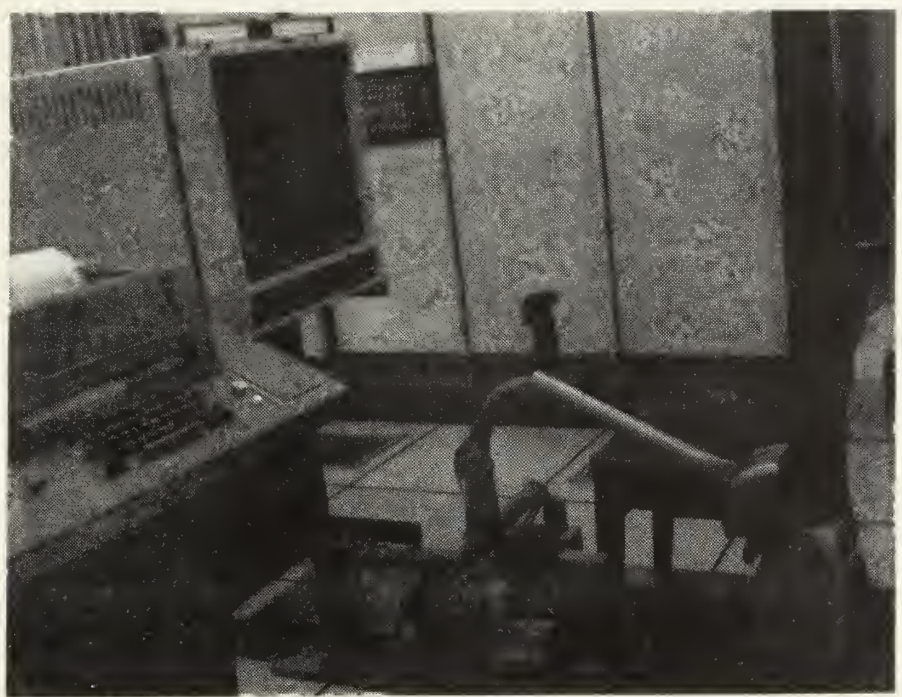
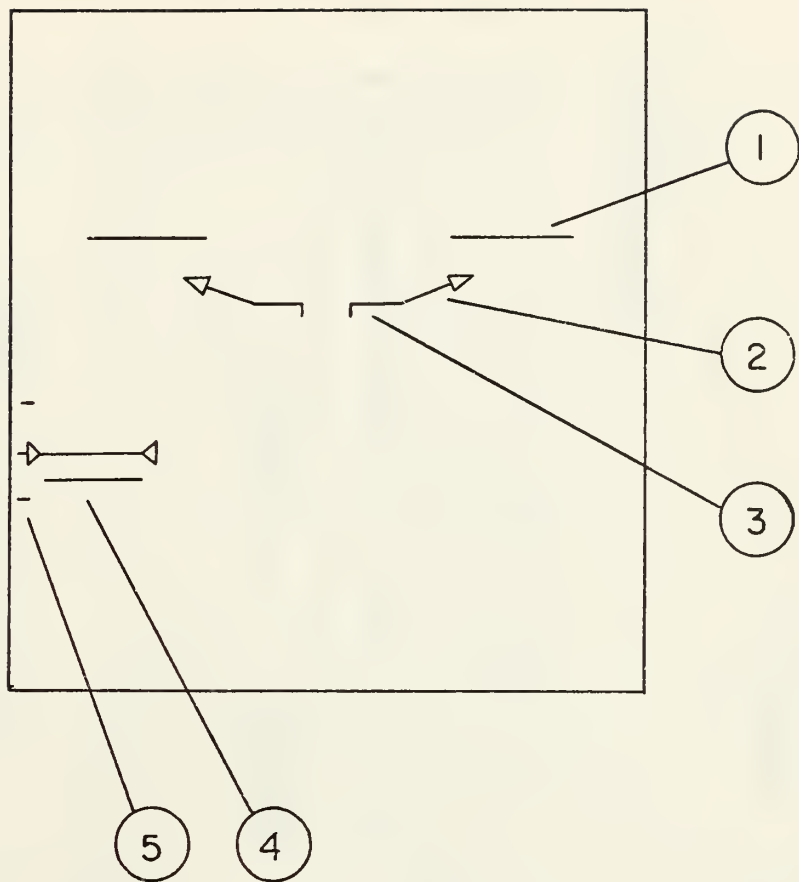


Figure 2. Apparatus.



Display Element	Situation	Units
1. horizon bar	pitch attitude	20 degrees/inch
2. airspeed indicaton	airspeed error	0.5 knots/degree
3. aircraft symbol	stationary	
4. glideslope bar	glideslope deviation	50 feet/inch
5. glideslope indicators	stationary	+ or - 50 feet

Figure 3. Cockpit display.

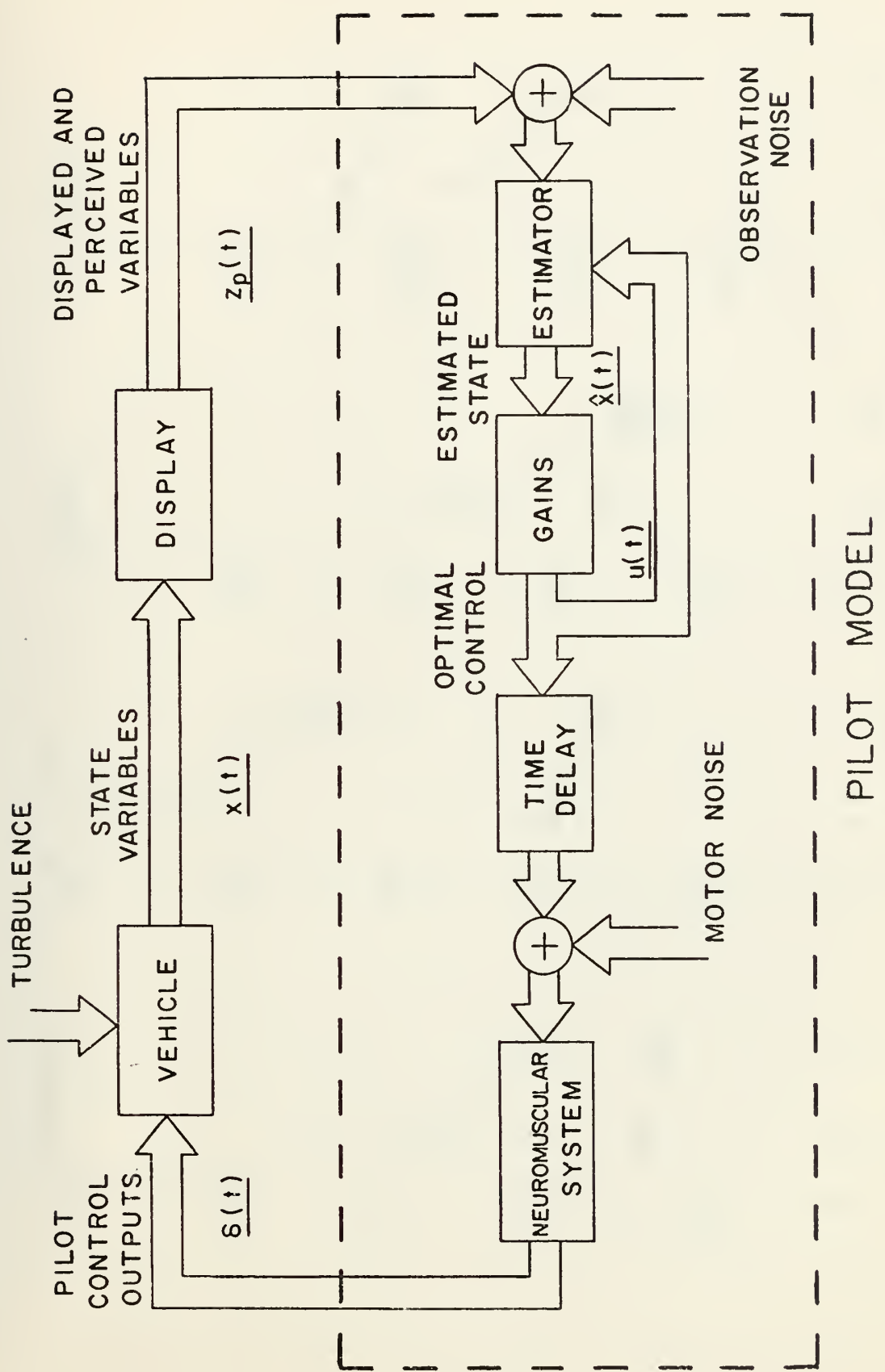
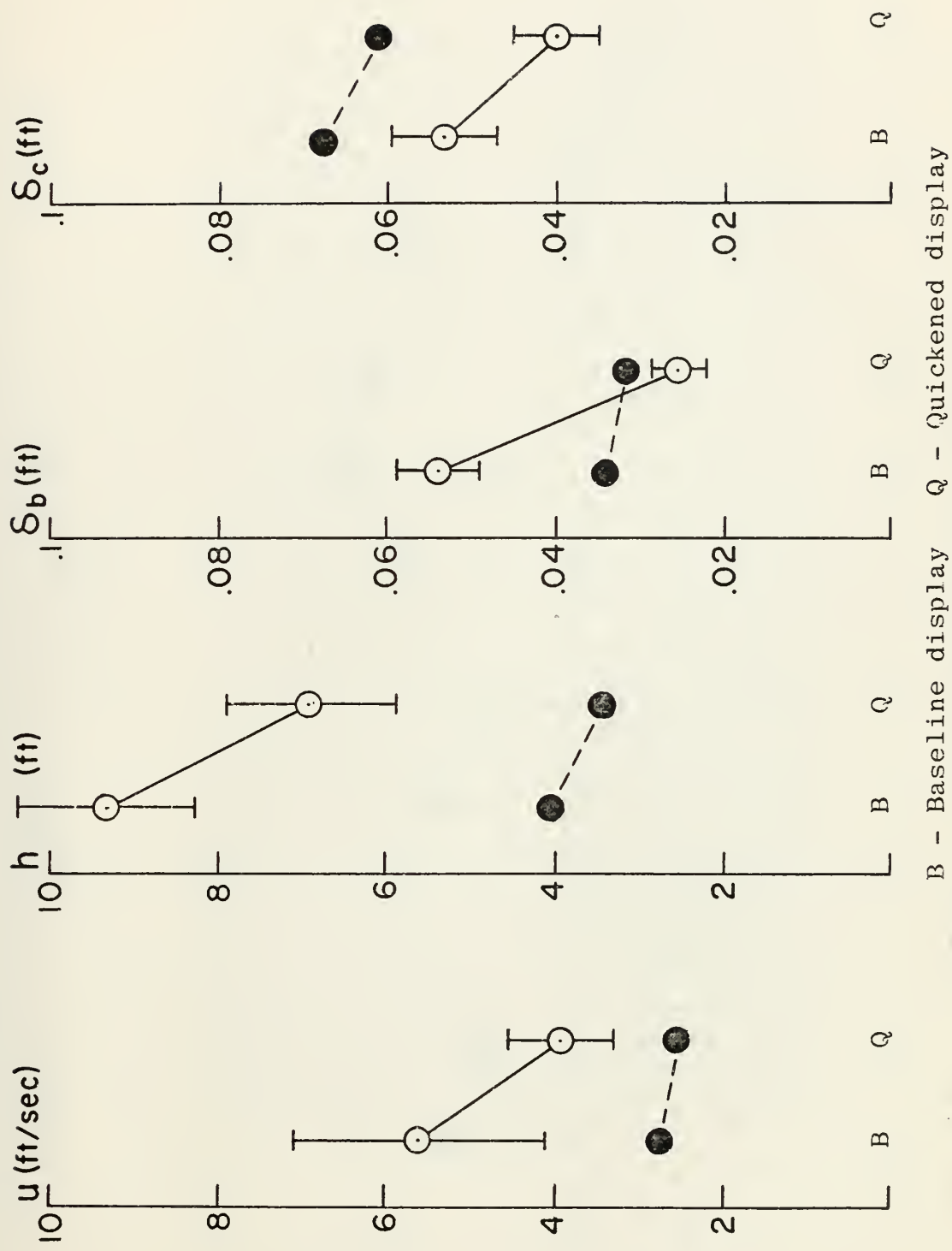


Figure 4. Optimal pilot model.



B - Baseline display Q - Quickened display

Figure 5. Performance values, subject A.

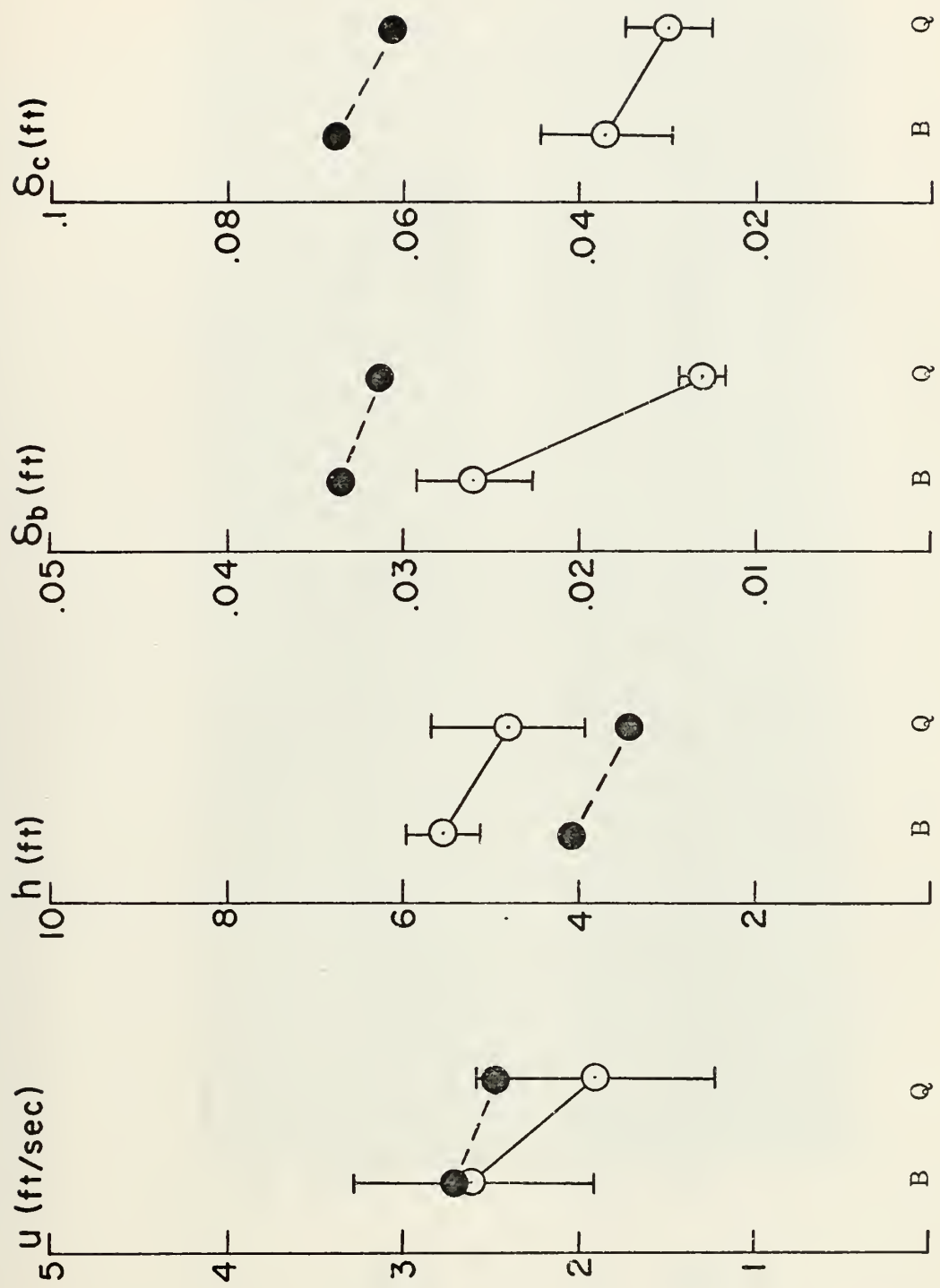


Figure 6. Performance values, subject B.

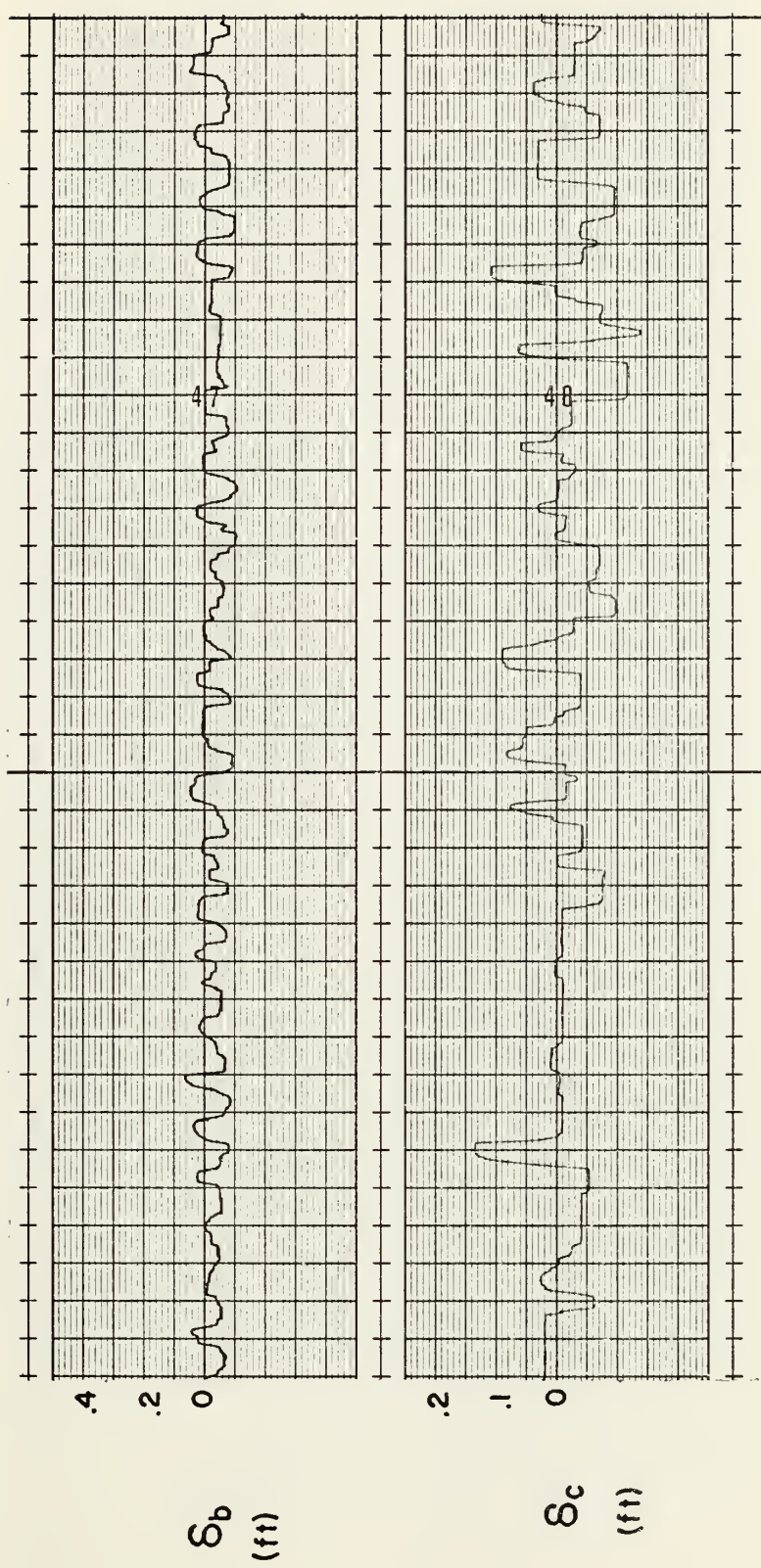


Figure 7. Control motion, baseline display.

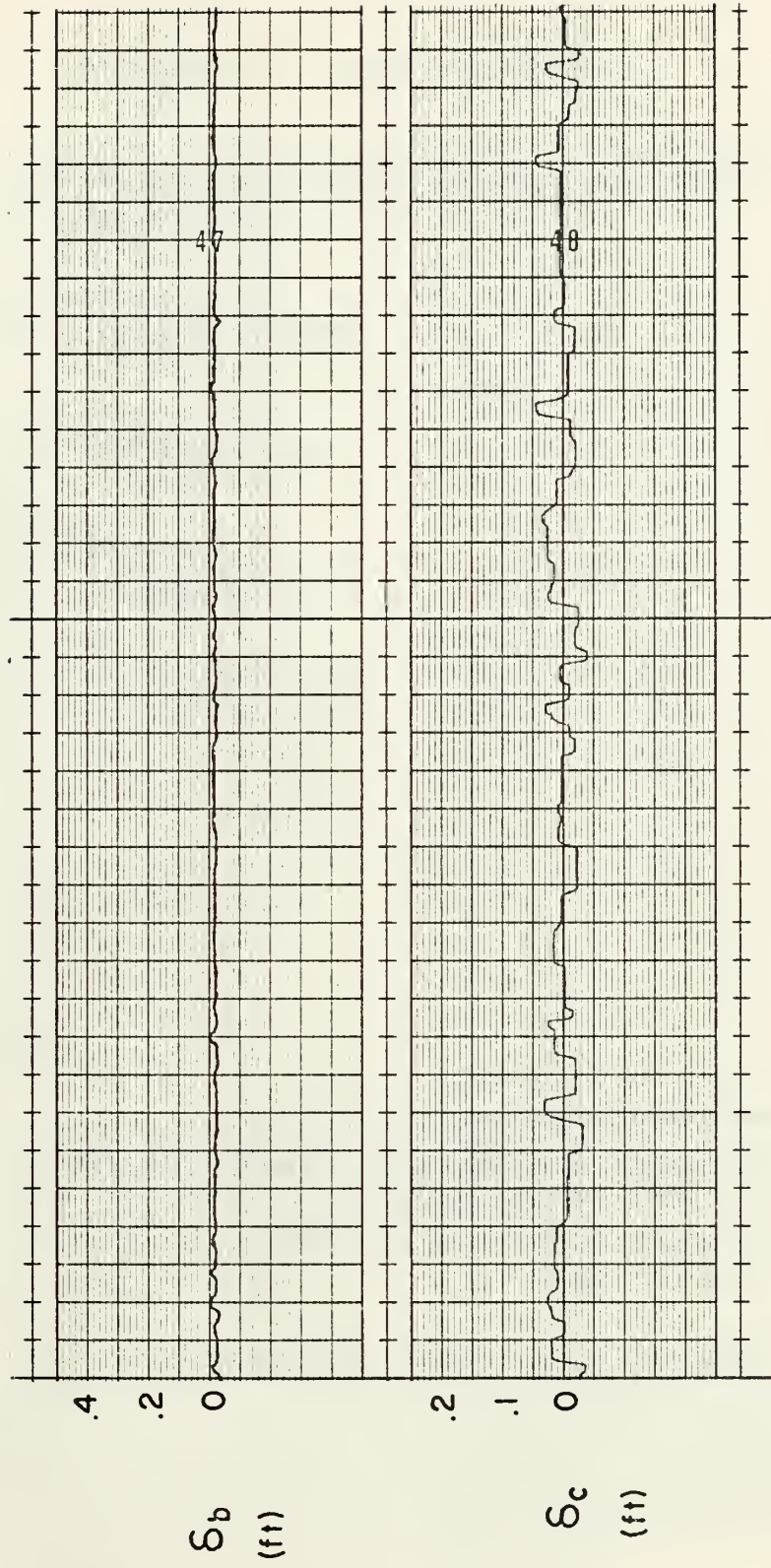


Figure 8. Control motion, quickened display.

APPENDIX A - DIGITAL PROGRAM

```
INTEGER IGD(6), FRAME(20), GSLP(12), ACREF(20), HORIZ(25)
DIMENSION ITD(60), ITEXT(12), UG(1000), WG(1000)
NAMELIST MODE, E16, E17, E21, E23, E24, E25
FRAME(1) = IHEAD(0,6)
*
DO 110 I=2,12
READ (5,270) X,Y, IDM
110 FRAME(I) = IPACK(X,Y, IDM)
GSLP(1) = IHEAD(0,7)
*
DO 120 I=2,11
READ (5,270) X,Y, IDM
120 GSLP(I) = IPACK(X,Y, IDM)
ACREF(1) = IHEAD(0,9)
*
DO 130 I=2,19
READ (5,270) X,Y, IDM
130 ACREF(I) = IPACK(X,Y, IDM)
HORIZ(1) = IHEAD(0,8)
*
DO 140 I=2,5
READ (5,270) X,Y, IDM
140 HORIZ(I) = IPACK(X,Y, IDM)
A1=4.472
A2=3.536
A3=2.236
A4=2.738
A5=2.236
CMU1=0.07
OMU2=0.21
OMU3=0.35
OMU4=0.768
OMU5=1.765
OMW1=0.42
OMW2=1.26
OMW3=2.1
OMW4=4.608
OMW5=10.05
UDR=9.95
*
*****
* TAKE CARE OF PERIPHERAL EQUIPMENT
*****
OUTPUT(102)'ENGAGE PATCHBOARDS, SELECT INPUT CONTROL, EXECUTE GATED, AND SET SENSE SWITCH'
OUTPUT(102)'SELECT SETTINGS FOR POTS 016,017,021,023,0124,025'
OUTPUT(102)'AS E16= ,E17= ,E21= ,E23= ,E24= ,E25= '
INPUT(101)
*
CALL SETPOT (4HP000,.0091,4HP001,.0053,4HP002,.0044,4HP004,.5680,4HP005,.5895,4HP006,.3000,4HP007,.5067,4HP0210,.9780,4HP011,.1689,4HP012,.0600,4HP013,.0178,4HP0143,.4732,4HP015,.1500,4HP020,.2534,4HP022,.6667,4HP027,.47880,4HP030,.6420,4HP031,.3552,4HP032,.6800,4HP033,.15569,4HP037,.0166,4HP042,.3099,4HP045,.1400,4HP050,.77256,4HP051,.0242,4HP052,.0815,4HP053,.1173,4HP054,.7077,47HP056,.4000,4HP057,.3500,4HP025,E25,4HP021,E21,4HP023,8E23,4HP024,E24,4HP016,E16,4HP017,E17)
IDEV = 1
145 IF(SENSESWITCH(1)) 155,150
150 IF(SENSESWITCH(2)) 152,145
152 IDEV=2
155 CONTINUE
```



```

CALL DGINIT (IDEV, IGD, 6, IER)
CALL DTINIT (IDEV, ITD, 50, IER)
160 OUTPUT(102)'SELECT DISPLAY MODE, MODE=1 OR 2'
INPUT(101)
ENCODE (48, 280, ITEXT)
CALL TEXT0 (IDEV, ITEXT, 12, 10, 1, 2, 2, IER)
ENCODE (48, 290, ITEXT)
CALL TEXT0 (IDEV, ITEXT, 12, 12, 1, 2, 2, IER)
ENCODE (48, 300, ITEXT)
CALL TEXT0 (IDEV, ITEXT, 12, 14, 1, 2, 2, IER)
ENCODE (48, 310, ITEXT)
CALL TEXT0 (IDEV, ITEXT, 12, 16, 1, 2, 2, IER)
ENCODE (48, 320, ITEXT)
CALL TEXT0 (IDEV, ITEXT, 12, 20, 1, 2, 2, IER)
ENCODE (48, 330, ITEXT)
CALL TEXT0 (IDEV, ITEXT, 12, 22, 1, 2, 2, IER)
ENCODE (48, 340, ITEXT)
CALL TEXT0 (IDEV, ITEXT, 12, 24, 1, 2, 2, IER)
T=0.0
*
DO 163 I=1,1000
SU1=OMU1*T
SU2=OMU2*T
SU3=OMU3*T
SU4=OMU4*T
SU5=OMU5*T
SW1=OMW1*T
SW2=OMW2*T
SW3=OMW3*T
SW4=OMW4*T
SW5=OMW5*T
UG(I)=(1./25.00)*(A1*SIN(SU1)+A2*SIN(SU2)+A3*SIN(SU3) +
1 A4*SIN(SU4)+A5*SIN(SU5))
WG(I)=(1./25.00)*(A1*SIN(SW1)+A2*SIN(SW2)+A3*SIN(SW3) +
1 A4*SIN(SW4)+A5*SIN(SW5))
T=T+(1.0/UDR)
163 CONTINUE
165 IF (TEST(1).GT.0) GO TO 165
CALL DTINIT (IDEV, ITD, 60, IER)
AB = 0.0
*
DO 170 I=6,10
HORIZ(I) = 0
J = I+7
FRAME(J) = 0
170 CONTINUE
IF (MODE.GT.1) GO TO 200
*****
* MODE 1, BASIC DISPLAY *
*****
CALL WRITECLOCK (0.)
CALL RESET (500)
CALL COMPUTE
CALL STARTCLOCK
*
DO 180 I=1,7200
CALL READCLOCK (V)
IF(V.GT.5400.0) GO TO 190
AB = AB+1.0
UG1=UG(I)
WG1=WG(I)
CALL DAC(1,UG1,2,WG1)
CALL ADK (0,AS,1,P,2,GS,3,Q,4,GSD)
P = .2865*p
GS = 0.4*GS
Y = .1-P
HORIZ(2) = IPACK(-.6,Y,0)
HORIZ(3) = IPACK(-0.125,Y,1)
HORIZ(4) = IPACK(0.125,Y,0)
HORIZ(5) = IPACK(.6,Y,1)
Y = -0.2-GS

```



```

GSLP(10) = IPACK(-0.57,Y,0)
GSLP(11) = IPACK(-0.37,Y,1)
GSLP(12) = IPACK(-0.57,Y,1)
ANGL = 0.7029*AS
SAN = SIN(ANGL)
CAN = COS(ANGL)
Y = 0.1*SAN+0.1
Y1 = Y+0.015
Y2 = Y-0.015
Y3 = 0.125*SAN+0.1
X = -0.1*CAN-0.125
X1 = X+0.015*SAN
X2 = X-C.015*SAN
X3 = -0.125*CAN-0.125
ACREF(2) = IPACK(X,Y,0)
ACREF(3) = IPACK(X1,Y1,1)
ACREF(4) = IPACK(X3,Y3,1)
ACREF(5) = IPACK(X2,Y2,1)
ACREF(6) = IPACK(X,Y,1)
X = -X
X1 = -X1
X2 = -X2
X3 = -X3
ACREF(15) = IPACK(X,Y,1)
ACREF(16) = IPACK(X2,Y2,1)
ACREF(17) = IPACK(X3,Y3,1)
ACREF(18) = IPACK(X1,Y1,1)
ACREF(19) = IPACK(X,Y,1)
CALL GRAPHO (IDEV,FRAME,20,1,IER)
CALL GRAPHO (IDEV,GSLP,12,2,IER)
CALL GRAPHO (IDEV,ACREF,20,3,IER)
CALL GRAPHO (IDEV,HORIZ,25,4,IER)
180 CONTINUE
190 CALL HOLD (500)
GO TO 260

```

```

*****
* MODE 2, QUICKENED DISPLAY
*****
200 CALL WRITECLOCK (0.)
CALL RESET (500)
CALL COMPUTE
CALL STARTCLOCK
*
DO 210 I=1,7200
CALL READCLOCK (V)
IF(V.GT.5400.0) GO TO 220
AB = AB+1.0
UG1=UG(I)
WG1=WG(I)
CALL DAC(1,UG1,2,WG1)
CALL ADK (0,AS,1,P,2,GS,3,Q,4,GSD)
P = .2865*(P+2.760*.4*Q)
GS = 0.4*(GS+.2*GSD)
Y = .1-P
HORIZ(2) = IPACK(-.6,Y,0)
HORIZ(3) = IPACK(-0.125,Y,1)
HORIZ(4) = IPACK(0.125,Y,0)
HORIZ(5) = IPACK(.6,Y,1)
Y = -0.2-GS
GSLP(10) = IPACK(-0.57,Y,0)
GSLP(11) = IPACK(-0.37,Y,1)
GSLP(12) = IPACK(-0.57,Y,1)
ANGL = 0.7029*AS
SAN = SIN(ANGL)
CAN = COS(ANGL)
Y = 0.1*SAN+0.1
Y1 = Y+0.015
Y2 = Y-0.015
Y3 = 0.125*SAN+0.1
X = -0.1*CAN-0.125
X1 = X+0.015*SAN

```



```

X2 = X-0.015*SAN
X3 = -0.125*CAN-0.125
ACREF(2) = IPACK(X,Y,0)
ACREF(3) = IPACK(X1,Y1,1)
ACREF(4) = IPACK(X3,Y3,1)
ACREF(5) = IPACK(X2,Y2,1)
ACREF(6) = IPACK(X,Y,1)
X = -X
X1 = -X1
X2 = -X2
X3 = -X3
ACREF(15) = IPACK(X,Y,1)
ACREF(16) = IPACK(X2,Y2,1)
ACREF(17) = IPACK(X3,Y3,1)
ACREF(18) = IPACK(X1,Y1,1)
ACREF(19) = IPACK(X,Y,1)
CALL GRAPHO (IDEV,FRAME,20,1,IER)
CALL GRAPHO (IDEV,GSLP,12,2,IER)
CALL GRAPHO (IDEV,ACREF,20,3,IER)
CALL GRAPHO (IDEV,HORIZ,25,4,IER)
210 CONTINUE
220 CALL HOLD (500)
*
260 CONTINUE
*
***** THIS SECTION TAKES INTEGRATED SQUARE VALUES FROM THE *
* ANALOG AND GIVES ROOT MEAN SQUARE PERFORMANCE VALUES. *
***** ****
CALL DGINIT (IDEV,IGD,6,IER)
CALL ADK(16,SAS,17,SGS,20,SDC,21,SDB,22,THD,23,THE)
CALL RESET (500)
SAS = SAS/(.104*E25)
SGS = SGS/(.012*E21)
SDC = SDC/(480.*E23)
SDB = SDB/(120.*E24)
THD = THD/(360.0*E17)
THE = THE/(2250.0*E16)
SAS = ABS(SAS)
SGS = ABS(SGS)
SDC = ABS(SDC)
SDB = ABS(SDB)
THD = ABS(THD)
THE = ABS(THE)
RMAS = SQRT(SAS)
RMGS = SQRT(SGS)
RMDC = SQRT(SDC)
RMDB = SQRT(SDB)
RMTD = SQRT(THD)
RMTH = SQRT(THE)
UDR = AB/120.0
WRITE (6,350) MODE
WRITE (6,360) UDR
WRITE (6,370) RMAS,RMGS,RMDB,RMDC,RMTD,RMTH
GO TO 160
*
270 FORMAT (2F10.4,I1)      THIS IS A HELICOPTER TRACKING
280 FORMAT ('1')             PROBLEM REQUIRING THE ADJUSTMENT OF
290 FORMAT ('1')             POWER AND PITCH ATTITUDE TO MAINTAIN
300 FORMAT ('1')             60 KTS ON A 6 DEGREE GLIDESLOPE.
310 FORMAT ('1')             WHEN READY TO BEGIN, PRESS THE
320 FORMAT ('1')             RED BUTTON ON THE COLLECTIVE LEVER.
330 FORMAT ('1')             THE TASK WILL LAST FOR 90 SECONDS.
340 FORMAT ('1')             'DISPLAY MODE ',I1/
350 FORMAT ('1','DISPLAY MODE ',I1/)

```



```
360 FORMAT ('0','UPDATE RATE AVERAGED ',F8.5,' TIMES PER S
1ECOND')
370 FORMAT ('0','RMS AIRSPEED           ',F8.5,' FT/SE
1C','0','RMS HEIGHT             ',F8.5,' FT','0',
2'RMS CYCLIC                  ',F8.5,' FT','0',
3'RMS COLLECTIVE              ',F8.5,' FT','0',
4'RMS VERTICAL TURBULENCE    ',F8.5,' FT/SEC','0',
5'RMS PITCH RATE               ',F8.5,' RAD/SEC','0',
6'RMS PITCH ANGLE              ',F8.5,' RAD ','/')

*
END
```

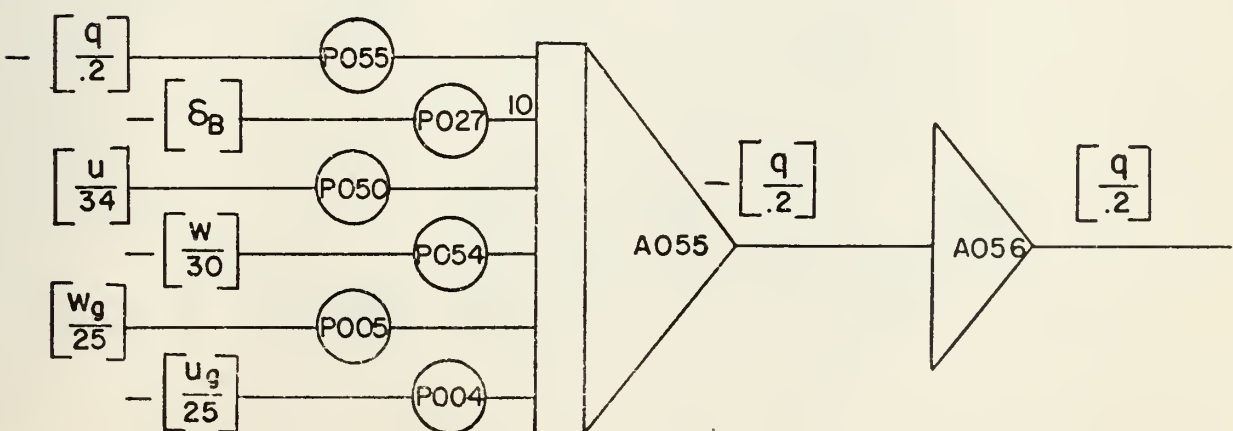
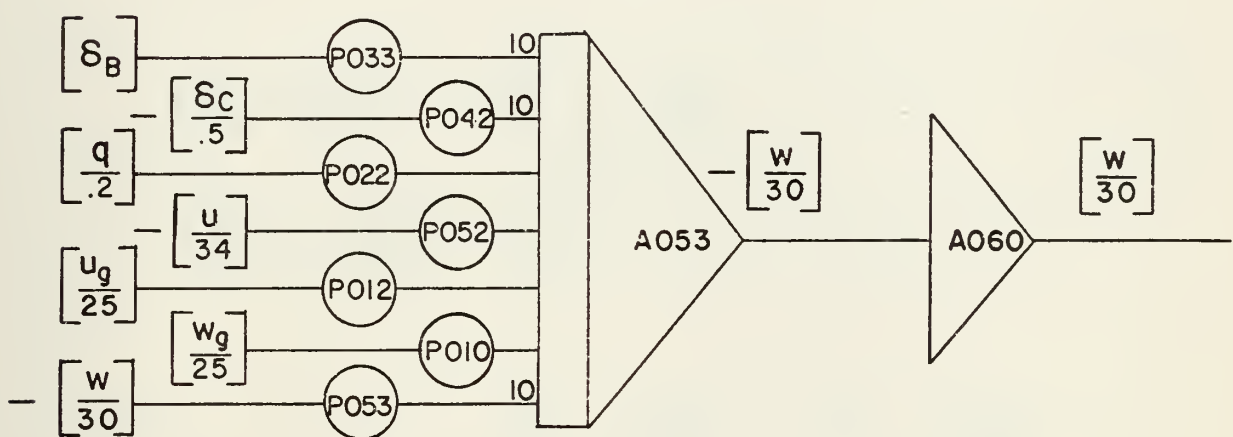
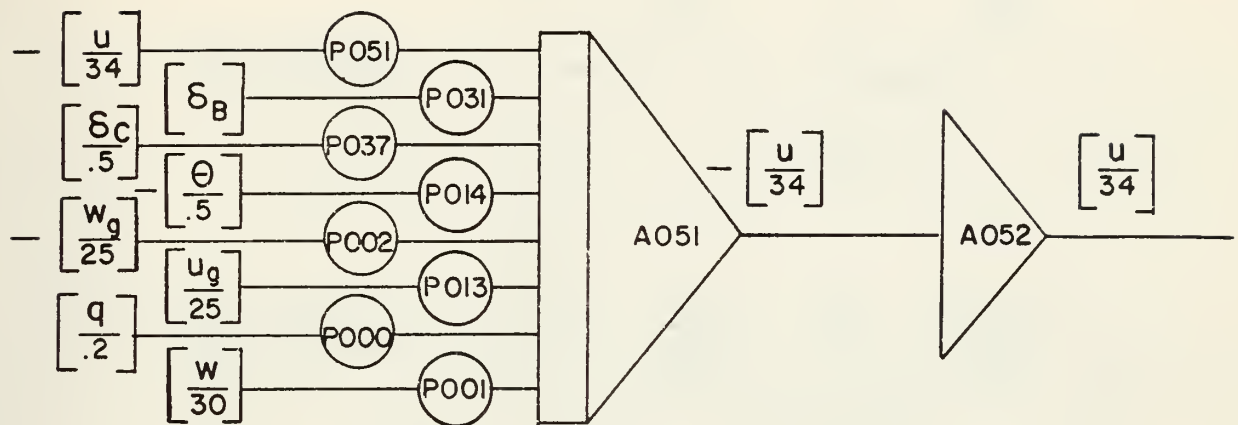

PROGRAM VARIABLES

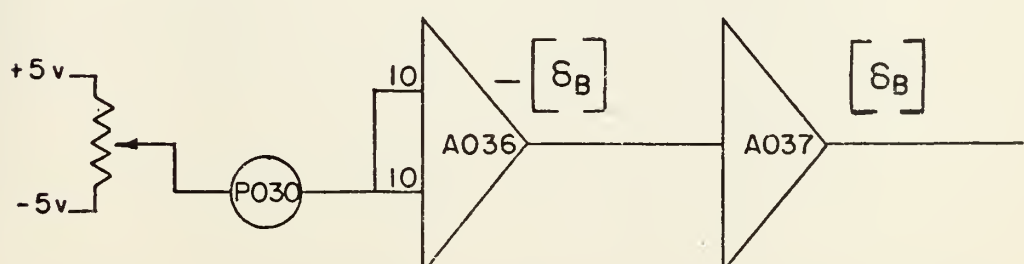
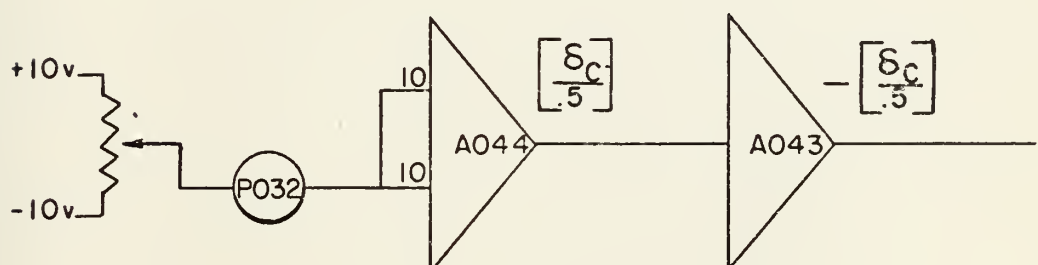
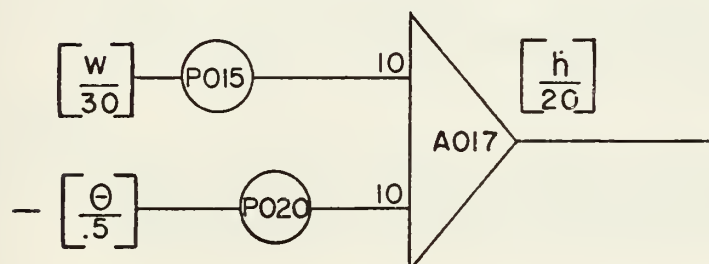
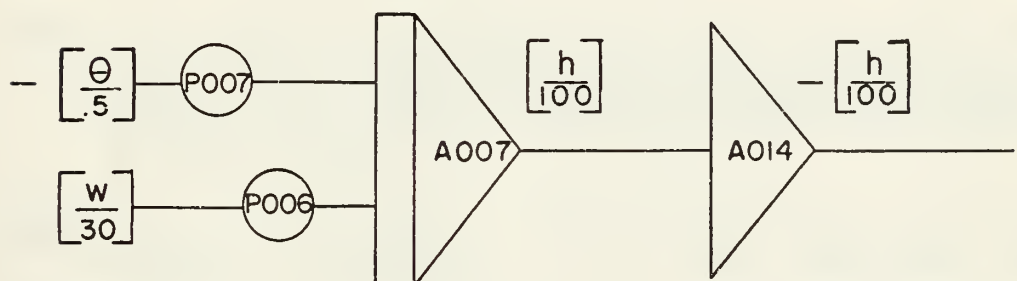
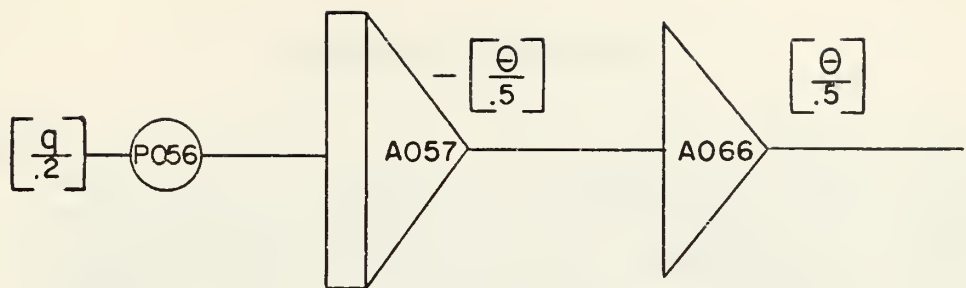
AB	Incremental number of display updates during simulation.
ACREF	Vector of coordinates defining aircraft reference.
ANGL	Angle defining airspeed deviation.
AS	Airspeed deviation.
CAN	Cosine of given angle.
E16	Setting for potentiometer 016.
E17	Setting for potentiometer 017.
E21	Setting for potentiometer 021.
E23	Setting for potentiometer 023.
E24	Setting for potentiometer 024.
E25	Setting for potentiometer 025.
FRAME	Vector of coordinates defining display frame.
GS	Glideslope (height) deviation.
GSD	Glideslope deviation rate.
GSLP	Vector of coordinates defining glideslope reference.
HORIZ	Vector of coordinates defining horizon reference.
IDEV	Graphics terminal in use, 1 or 2.
IDM	Graphics instruction, draw or move.
IER	Error type code.
IGD	Graphics instruction, size of graphics input.
ITD	Graphics instruction, size of text input.
ITEXT	Vector of text input.
MODE	Display mode, 1 or 2.
P	Pitch angle.

Q	Pitch rate.
RMAS	Root mean square airspeed deviation.
RMDB	Root mean square cyclic movement.
RMDC	Root mean square collective movement.
RMGS	Root mean square glideslope deviation.
RMTD	Root mean square pitch rate.
RMTE	Root mean square pitch angle.
SAN	Sine of given angle.
SAS	Mean square airspeed deviation.
SDB	Mean square cyclic movement.
SDC	Mean square collective movement.
SGS	Mean square glideslope deviation.
T	Time increment.
THD	Mean square pitch rate.
THE	Mean square pitch angle.
UDR	Update rate for the 90 second period.
UG	Vector of horizontal turbulence magnitudes.
UG1	Specific horizontal turbulence value.
WG	Vector of vertical turbulence magnitudes.
WG1	Specific vertical turbulence value.
V	Internal clock count, 60 cycles per second.
X	Running variable, abscissa.
Y	Running variable, ordinate.
A1,A2,...A5	Sine wave magnitudes.
OMU1,OMU2,...OMU5	Horizontal turbulence frequencies.
OMW1,OMW2,...OMW5	Vertical turbulence frequencies.

SU1,SU2,...,SU5 Sine values for horizontal turbulence.
SW1,SW2,...,SW5 Sine values for vertical turbulence.

APPENDIX B - ANALOG PROGRAM





LIST OF REFERENCES

1. Murphy, M.R., McGee, L.A., Palmer, E.A., Paulk, C.H., and Wempe, T.E., "Simulator Evaluation of Three Situation and Guidance Displays for V/STOL Zero-Zero Landings," Proceedings of the Xth Annual Conference on Manual Control, Air Force Institute of Technology / Air Force Flight Dynamics Laboratory, p. 439, April 1974.
2. National Aeronautics and Space Administration Technical Note D-5913, Fixed-Base Simulation Evaluation of Various Low-Visibility Landing Systems for Helicopters, by P.S. Rempfer, L.E. Stevenson, and J.S. Koziol, Jr., March 1971.
3. McRuer, D., "Development of Pilot-in-the-Loop Analysis," Journal of Aircraft, v. 10, p. 515, September 1973.
4. Air Force Systems Command Technical Documentary Report Number ASD-TDR-62-347, Stochastic Disturbance Data for Flight Control Systems Analysis, By J.E. Hart, L.A. Adkins, and L.L. Lacau, September 1962.
5. National Aeronautics and Space Administration Contractor Report 1952, Analytic Evaluation of Display Requirements for Approach to Landing, by D.L. Kleinman and S. Baron, November 1971.

INITIAL DISTRIBUTION LIST

	No. Copies
1. Library, Code 0212 Naval Postgraduate School Monterey, California 93940	2
2. Department Chairman, Code 57 Department of Aeronautical Engineering Naval Postgraduate School Monterey, California 93940	1
3. Asst Proffessor R. A. Hess, Code 57He Department of Aeronautical Engineering Naval Postgraduate School Monterey, California 93940	1
4. LT Luther William Wheat, USN ANTARTICDEVRON SIX Point Mugu, California 93042	1
5. Defense Documentation Center Cameron Station Alexandria, VA 22314	2

Thesis
W4843 Wheat
c.1

102274

A comparison of optimal control theory predictions with actual pilot performance in a helicopter longitudinal tracking task.

Thesis
W4843 Wheat
c.1

102274

A comparison of optimal control theory predictions with actual pilot performance in a helicopter longitudinal tracking task.

thesW4843

A comparison of optimal control theory p



3 2768 001 95031 4

DUDLEY KNOX LIBRARY